STEM CELLS AND DEVELOPMENT
Volume 23, Number 24, 2014

DOI: 10.1089/scd.2014.0064

Sphere Formation Permits Oct4 Reprogramming of Ciliary Body Epithelial Cells into Induced Pluripotent Stem Cells

Aiguo Ni, Ming Jing Wu, and Sai H. Chavala

Somatic cells can be reprogrammed to induced pluripotent stem (iPS) cells by defined sets of transcription factors. We previously described reprogramming of monolayer-cultured adult mouse ciliary body epithelial (CE) cells by Oct4 and Klf4, but not with Oct4 alone. In this study, we report that Oct4 alone is sufficient to reprogram CE cells to iPS cells through sphere formation. Furthermore, we demonstrate that sphere formation induces a partial reprogramming state characterized by expression of retinal progenitor markers, upregulation of reprogramming transcription factors, such as Sall4 and Nanog, demethylation in the promoter regions of pluripotency associated genes, and mesenchymal to epithelial transition. The Oct4-iPS cells maintained normal karyotypes, expressed markers for pluripotent stem cells, and were capable of differentiating into derivatives of all three embryonic germ layers in vivo and in vitro. These findings suggest that sphere formation may render somatic cells more susceptible to reprogramming.

Introduction

The ciliary body is a region that harbors ocular cells that are easily surgically accessible, and are of interest for regenerative ophthalmology [1–4]. The surface of the ciliary body is composed of a series of ridges called ciliary processes. The ciliary processes are covered by a specialized epithelium that is of neuroepithelial origin.

Sphere formation assays in a serum-free medium were first described as a method to select and expand stem cells [5,6]. Previous studies demonstrated that primary ciliary body epithelial (CE) cells have the ability to form clonal neurospheres, suggesting stem cells-like cells residing in the ciliary body epithelium [7]. CE sphere-derived cells expressed some retinal stem/progenitor cell markers in the culture [7,8]. However, the expression seems to be induced by growth factors in the medium. It remains unclear if these cells are bona fide quiescent retinal stem cells [8,9].

Generation of induced pluripotent stem (iPS) cells through ectopic expression of defined transcription factors holds great potential for regenerative medicine and disease modeling [10]. We previously found that mouse CE-derived cells, grown in monolayer cultures, express Sox2, Klf4, and c-Myc, and that these monolayer CE cells can be reprogrammed into iPS cells with ectopic Oct4 and Klf4 (2F), but not with Oct4 alone [1]. Given that adult neural stem cells, capable of sphere formation, have been previously reprogrammed into iPS cells with Oct4 alone [11,12], and that CE cells have the remarkable plasticity to form spheres displaying certain characteristics of neuroepithelial progenitors [7,8], we attempted to reprogram CE sphere-derived cells with Oct4 alone.

Materials and Methods

Animals

All procedures on mice were performed in accordance with the ARVO Statement for the Use of Animals in Ophthalmic and Vision Research and approved by the Institutional Animal Care and Use Committee at the University of North Carolina at Chapel Hill. Wild-type (WT) CD-1 strain mice, aged 5–6 weeks, were used for the study.

CE spheres and monolayer cultures

Dissection of adult mouse ciliary body was performed as previously described [7]. Dissociated cells were resuspended in a serum-free growth medium (SFM) containing Neurobasal medium, 1× B27 supplement, 1% penicillin/streptomycin, 2 mM L-glutamine, 20 ng/mL basic fibroblast growth factor (Peprotech), 20 ng/mL epidermal growth factor (Peprotech), and 2 μg/mL heparin (Sigma). To generate floating spheres, CE cells were plated at a density of 20 cells per microliter in ultra-low attachment 24-well plates (Corning) [8]. To establish monolayer cultures, cells were grown in SFM supplemented with 1% fetal bovine serum

Department of Ophthalmology, University of North Carolina, Chapel Hill, North Carolina.

(FBS) as previously described [1]. The medium was changed every 3 days. All cell culture reagents were from Invitrogen, unless otherwise noted.

Induction of iPS cells

The procedure of iPS cells generation was essentially as previously described with minor modifications [1]. In brief, all spheres at day 7 were dissociated into single cells with Accutase (Sigma) and plated at 1×10^5 cells per well of gelatin-coated six-well plates in 1% FBS-containing SFM. CE monolayer cultures at passage 2 (7 days after isolation) were plated the same as above. The next day, for the two-factor transduction, concentrated lentiviruses containing CMV promoter-driven human Oct4 and Klf4 or Sall4 (Cellomics Technology) were added to the cells at a multiplicity of infection of 10 with 4 μg/mL polybrene (Sigma) in 1% FBS-containing SFM, whereas for the one-factor transduction, only lentivirus coding human Oct4 was added. Twenty-four hours post infection, the viral infection mix was exchanged for fresh 1% FBS-containing SFM. The following day, transduced cells were subcultured onto mitomycin C-treated SNL feeder cells (Cell Biolabs) in six-well plates at a split ratio of 1:4 in embryonic stem (ES) cell medium minus leukemia inhibitory factor (LIF) containing Dulbecco's modified Eagle's medium (DMEM) supplemented with 15% FBS, 2 mM L-glutamine, 100 μM non-essential amino acids, 100 μM 2-mercaptoethanol, 50 U/mL penicillin, and 50 μg/mL streptomycin [13]. At day 21, the ES cell medium was replaced with serum-free N2B27 medium supplemented with LIF and 2i inhibitors [14], CHIR99021 (3 μM; Stemgent), and PD0325901 (1 μM; Stemgent). After another 7 days, ES cell-like colonies were picked and dissociated with trypsin and expanded on SNL feeders in KnockOut DMEM supplemented with 15% knockout serum replacement (KSR), 100 μM minimum essential medium (MEM) non-essential amino acids, 100 μM 2-mercaptoethanol, 2 mM L-glutamine, 50 U penicillin, and 50 μg/mL streptomycin [15].

The efficiency of generating iPS cells was calculated by dividing the number of alkaline phosphatase (or Nanog)-positive ES cell-like colonies by the seeded cell number.

Viral vector integration analysis

Genomic DNA was isolated with the Quick-gDNA MiniPrep (Zymo Research) according to the manufacturer's instructions. Genomic polymerase chain reaction (PCR) was performed as previously described [1].

Karyotyping

Karyotyping was performed by KaryoLogic, Inc. (http://karyologic.com/).

Bisulfite genomic sequencing

Bisulfite sequencing and DNA methylation analysis was performed as previously described [1]. Briefly, genomic DNA was prepared with Quick-gDNA MiniPrep (Zymo Research) and treated with the EZ DNA Methylation-Lightning Kit (Zymo Research) according to the manufacturer's instructions. Previously published nested primer sets were used to amplify the promoter regions of the genes: Sox2, Nanog, and Oct4 [16,17]. Amplified fragments were cloned using the Zero Blunt TOPO PCR Cloning Kits (Invitrogen). Individual clones (10 or more) were sequenced with the SP6 and T7 primers.

RNA isolation, reverse transcription–polymerase chain reaction, and real-time PCR

Total RNA was isolated from the cells with the Direct-zol RNA MiniPrep (Zymo Research) with DNase I digestion. Total RNA of mouse ES-D3 cell line was purchased from Cell Biolabs. Complementary DNA was synthesized with Superscript III First-Strand Synthesis System (Invitrogen). PCR and Real-time PCR were performed as previously described [1]. Previously published primer sets were used [1,9,18,19]. The mRNA level of target gene was normalized to the housekeeping gene HPRT.

Immunofluorescence staining and alkaline phosphatase staining

Immunofluorescence staining was performed as previously described [1]. Briefly, fixed cells were treated with a blocking solution, followed by an overnight incubation with the primary antibodies at 4°C. After rinsing with phosphate-buffered saline, the cells were incubated with secondary antibodies, rinsed and counter-stained with Hoechst 33342. iPS cells were also stained with an Alkaline Phosphatase Staining Kit (Stemgent) following the manufacturer's instructions.

In vitro differentiation and teratoma formation

In vitro differentiation and teratoma formation were performed as previously described [1].

Statistics

In all real-time PCR experiments, $n = 3$. P-value was calculated using the Student's t-test.

Results/Discussion

We isolated CE cells from ciliary body of CD1 WT mice, and cultured them as free-floating spheres in SFM (Fig. 1A). In agreement with previous studies [7–9], our reverse transcription–polymerase chain reaction (RT-PCR) analysis revealed that the expression of retinal progenitor markers such as Pax6, Sox2, Rax, Otx2, Lhx2, Six3, and nestin were induced in the culture in the sphere and monolayer cells, whereas differentiated ciliary epithelial marker Palmdelphin (Palmd) remained stable in the sphere, but decreased in the monolayer, and another ciliary epithelial transcript Tyrosinase (Tyr) decreased progressively in the sphere and monolayer (Fig. 1B). Together, these results suggested that CE cells acquired neural progenitor properties following culturing in mitogen-containing SFM.

Next, we reprogrammed CE sphere-derived cells with ectopic Oct4 and Klf4 (2F), and with Oct4 alone (Fig. 2A). At day 21 after infection, we observed ES cell-like colonies in 2F-transduced CE sphere-derived cells and about 44 alkaline phosphatase-positive colonies (44/100,000) after another 7 days, with a reprogramming efficiency close to the 2F control experiment using CE monolayer culture as described previously [1]. However, with Oct4 alone, no iPS

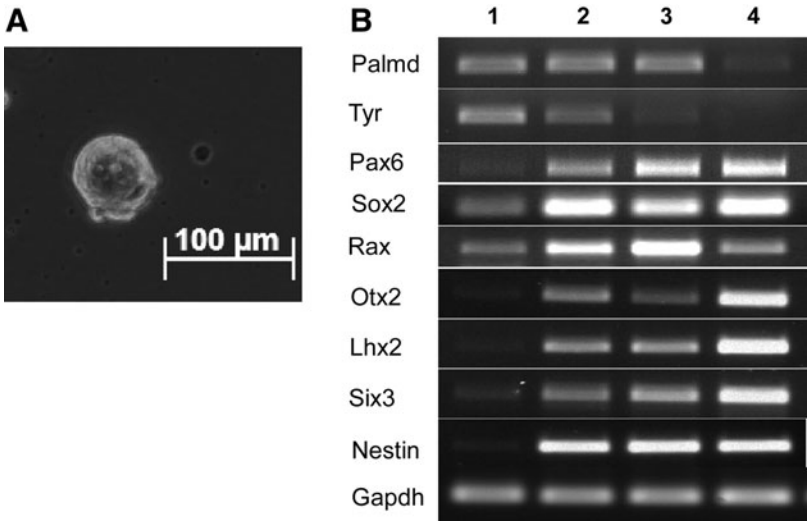

FIG. 1. Mouse ciliary body epithelial (CE) cell culture. **(A)** Brightfield image of a 7-day old CE sphere. **(B)** Reverse transcription–polymerase chain reaction (RT-PCR) showed that the expression of retinal progenitor markers, Pax6, Sox2, Rax, Otx2, Lhx2, Six3, and nestin, were induced in culture in the sphere and monolayer cells, whereas the differentiated CE marker Palmd remained stable in the sphere, but decreased in the monolayer, and another CE transcript Tyr decreased progressively in the sphere and monolayer (*lane* 1, CE tissue; *lane* 2, 4-day old sphere; *lane* 3, 7-day old sphere; *lane* 4, 7-day old monolayer).

cell colonies emerged, even after another 14 days. As described previously in the 1F experiment using CE monolayer culture, some morphological changes occurred, suggesting a partially reprogrammed state. When switching to serum-free N2B27 medium with dual inhibition (2i) of glycogen synthase kinase-3 and mitogen-activated protein kinase signaling at day 21 post infection, one ES cell-like colony (Fig. 2B, left) appeared at day 28 after infection from 100,000 seeded CE sphere-derived cells, with a reprogramming efficiency of 0.001% at day 35 (1/100,000, three times). In contrast, in the parallel 1F experiment using CE monolayer culture, iPS cell colonies were never observed, even with more initially plated cells (Fig. 2B, right, $0/10^6$, two times).

All of the three picked 1F colonies could be further expanded for more than 20 passages in serum-free N2B27 medium supplemented with 2i/LIF, displaying proliferation and a morphology characteristic of ES cells (Fig. 3A) and

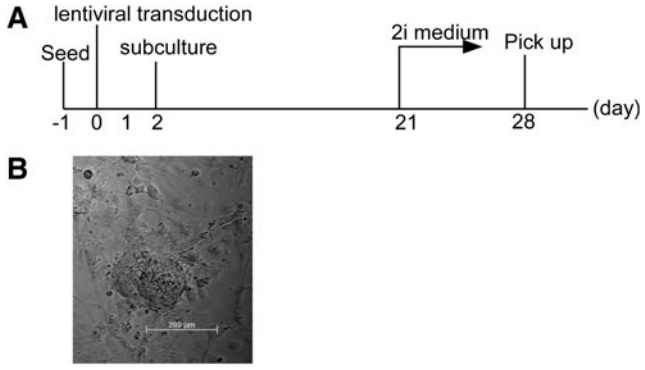

FIG. 2. Generation of induced pluripotent stem (iPS) cells from CE sphere-derived cells with reprogramming factor Oct4. **(A)** Timeline for reprogramming CE sphere-derived cells into iPS cells. CE sphere-derived cells were transduced with Oct4. Transduction mix was exchanged for fresh growth medium at day 1. At day 2 transduced cells were subcultured onto SNL feeder cells in embryonic stem cell medium minus leukemia inhibitory factor (LIF). At day 21, the medium was switched to 2i-medium. **(B)** Representative 1F iPS colony from CE sphere-derived cells (*left*) and negative control from CE monolayer (*right*).

maintaining alkaline phosphatase activity (Fig. 3B). 1F-iPS cells were confirmed to have only Oct4 transgene by genomic PCR (Fig. 3C), suggesting that ectopic Sox2, Klf4, and c-Myc are dispensable for reprogramming CE sphere-derived cells into iPS cells. The established 1F-iPS cell lines were then further characterized. They expressed all tested endogenous pluripotency markers, as detected by RT-PCR (Fig. 3D), whereas the transgene hOct4 was significantly attenuated at late passages (Fig. 3E). With immunofluorescence staining, we confirmed transcription markers such as Oct4, Sox2, and Nanog, and pluripotent cell surface marker SSEA-1 (Fig. 3F). DNA methylation pattern in Oct4 and Nanog promoters in 1F-iPS cells were similar to that in embryonic stem cells (ESCs) (Fig. 3G). In addition, 1F-iPS cells maintained a normal karyotype (Fig. 3H). We next evaluated the differentiation potential of 1F-iPS cells in vitro. 1F-iPS cells effectively formed embryoid bodies (EB) (Fig. 3I). Ten days after EB transfer onto gelatin-coated plates, the attached cells expressed markers of three germ layers, including the ectoderm markers Nefl and Nestin, the mesoderm markers KDR, FLT1, and T (Brachyury), and the endoderm markers Foxa2 and GATA4 as determined by RT-PCR (Fig. 3J). To fully characterize the differentiation potential in vivo, we injected 1F iPS cells into immune-deficient NOD-SCID mice. Histological examinations showed that the generated teratomas contained derivatives of all three embryonic germ layers (Fig. 3K). We confirmed these morphological findings with immunofluorescence staining: neural epithelial-like tissues (ectoderm) were positive for tubulin-β III expression, muscle-like tissues (mesoderm) were positive for α-smooth muscle actin, and gut-like epithelium (endoderm) was positive for E-cadherin expression (Fig. 3L). These observations suggested that the 1F iPS cells were fully reprogrammed into pluripotency.

To better understand why sphere formation makes CE cells amendable to 1F reprogramming, we evaluated mRNA expression of some key pluripotency-associated genes and genes involved in mesenchymal–epithelial transition (MET) by quantitative RT-PCR (Fig. 4A). Neither the CE sphere nor the monolayer culture expresses Oct4 at appreciable levels. Sox2 expression was high, but almost at the same level. Although Prdm14, Esrrb, and Dppa2 expression was

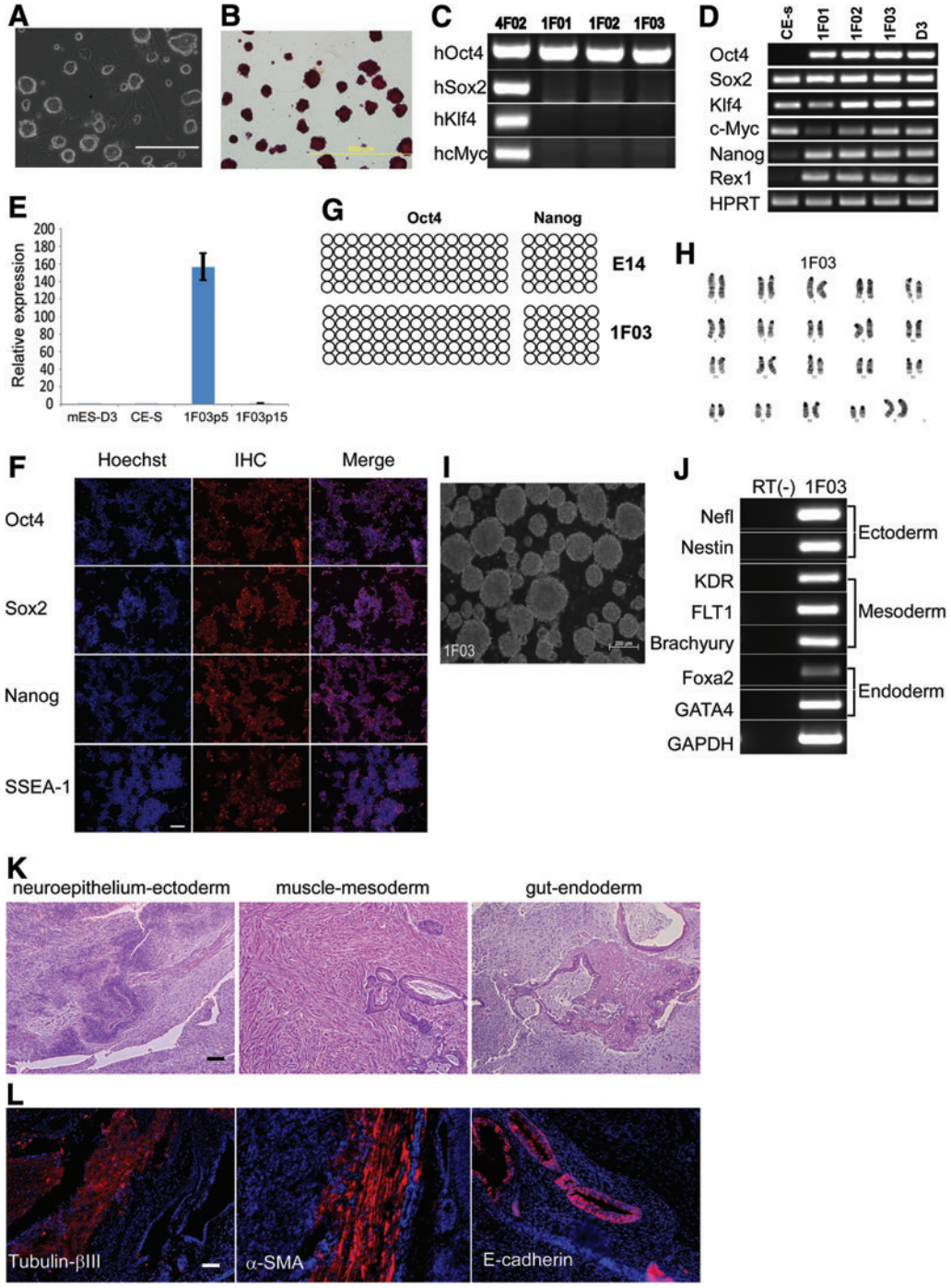

FIG. 3. Characterization of 1F iPS cells. **(A)** Representative 1F-iPS cell line cultured in the N2B27 + 2i/LIF medium. **(B)** Alkaline phosphatase staining of representative 1F-iPS cell line. **(C)** Genotyping of 1F iPS cells. Genomic PCR showed only Oct4 transgene in the three 1F-iPS cell lines (1F01, 1F02, and 1F03) as expected. 4F-iPS cells (4F02) were used as control. **(D)** RT-PCR of pluripotency-associated genes and HPRT. 1F-iPS cells express all tested endogenous pluripotency genes as mouse embryonic stem cells (D3), and parental CE sphere-derived cells (CE-s) express Sox2, Klf4, and c-Myc. **(E)** Expression of the transgene hOct4 is significantly attenuated in late passage 1F03 iPS cells. RT-quantitative PCR for the mRNA of viral hOct4 in wild-type CE sphere (CE-S), mouse ES D3 line, and 1F03 iPS cells at passage 5 (1F03p5) and passage 15 (1F03P15). **(F)** Immunostaining of pluripotency markers Oct4, Sox2, Nanog, and SSEA-1 in 1F03 iPS cells. Scale bar, 100 μm. **(G)** Methylation analysis of the Oct4 and Nanog promoters in ES (E14) and 1F03 iPS cells. Bisulfite sequencing of the Oct4 and Nanog promoters revealed that CpGs in the parental CE cells (Fig. 4B) were converted to a demethylated state in the 1F03 iPS cells resulting in a methylation pattern similar to that of mouse ES cells. *Open circles* indicate unmethylated CpG. **(H)** Karyotyping analysis of 1F03 iPS cells revealed their female karyotypes with normal chromosomal stability/integrity. **(I)** Embryoid bodies derived from 1F03 iPS cells. **(J)** RT-PCR of typical lineage markers after differentiation of embryoid bodies from 1F03F iPS clones. **(K)** Teratoma formation. Hematoxylin and eosin staining of teratoma sections derived from 1F iPS clones showed all three embryonic germ layers. **(L)** Immunostaining of teratoma sections showed tubulin-β III positive neural epithelium, α-smooth muscle actin-positive muscle and E-cadherin-positive endodermal cells. Scale bar, 100 μm. Color images available online at www.liebertpub.com/scd

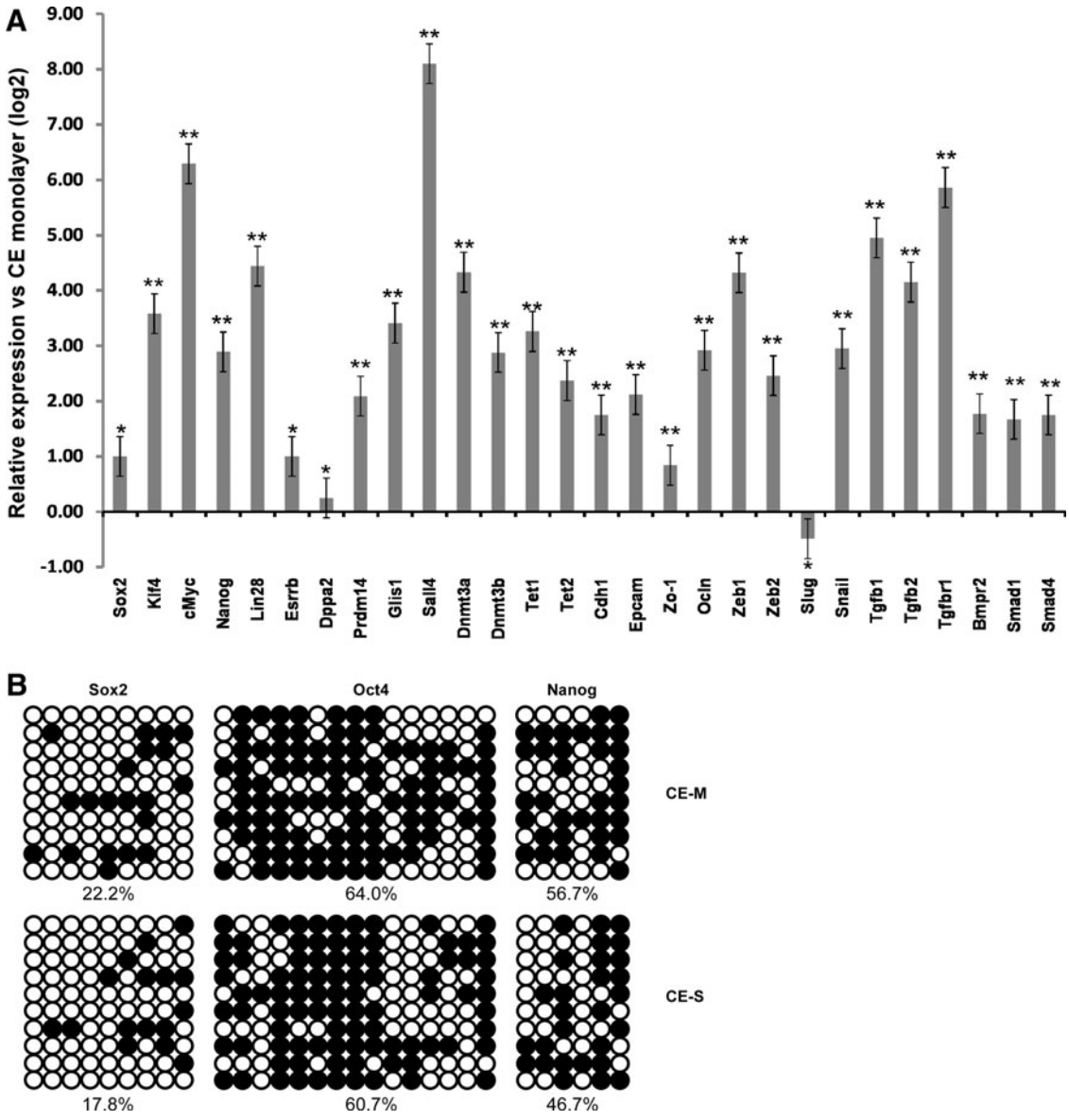

FIG. 4. Gene expression in the CE sphere and monolayer. **(A)** Quantitative real-time PCR was performed on the primary CE sphere (7 days old) and CE monolayer (passage 2 at 7 days after isolation). Neither of the cells expresses Oct4 at appreciable levels. Compared with the CE monolayer (set as 0), expression levels of Sox2, Klf4, c-Myc, Nanog, Lin28, Esrrb, Dppa2, Prdm14, Glis1, Sall4, Dnmt3a, Dnmt3b, Tet1, Tet2, Cdh1, Epcam, Zo-1, Ocln, Zeb1, Zeb2, Snail, Tgfb1, Tgfb2, Tgfbr1, Bmpr2, Smad1, and Smad4 are increased in the CE sphere. Data are normalized for HPRT expression and presented as mean ± standard error of the means for three replicates. **P* value < 0.05; ***P* value < 0.01. **(B)** Methylation patterns of the Sox2, Nanog, and Oct4 gene promoters were analyzed using bisulfate-treated DNA from the CE sphere (CE-S) and the CE monolayer (CE-M). *Closed circles* indicate methylated CpG and *open circles* indicate unmethylated CpG.

increased, the expression levels of Sall4, c-Myc, Lin28, Glis1, Klf4, and Nanog were most significantly upregulated in the sphere compared with the monolayer. Combination of these factors with or without Oct4 has been shown to successfully reprogram mouse embryonic fibroblasts to iPS cells [20–22]. Recently, Sall4 was identified as one of the two most induced genes (the other Sox2) in the early phase in response to the seven small molecule combination in a chemical reprogramming that efficiently drives iPS cells reprogramming in mouse somatic cells [18]. To assess whether Sall4 could enhance 1F-Oct4 reprogramming, we asked if overexpression of Sall4 in the CE monolayer with Oct4 could generate iPS cells. Surprisingly, we did not observe any ES-like colonies, which we performed twice. This suggests that additional mechanisms are responsible for the reprogramming advantage observed with CE spheres. Since we determined that CE monolayer could be reprogrammed with 2F (Klf4 and Oct4), we propose that upregulation of Klf4, or genes that can replace Klf4 function, can circumvent the requirement of Klf4. Indeed we found that Klf4, and Esrrb, Glis1 and Prdm14, which have been shown to replace Klf4 in reprogramming [21,23,24], were upregulated by CE sphere formation. Whether the upregulation of these genes is responsible for 1F-Oct4 reprogramming of CE sphere-derived

cells requires further investigation. It is, however, tempting to speculate that one step of sphere formation might reduce the small molecule number and speed up the reprogramming process in a chemical reprogramming of CE spheres since Sox2 expression is already high or induced by sphere formation (Figs. 1B and 3D). Two de novo DNA methyltransferases, Dnmt3a and Dnmt3b, and the 10–11 Translocation-family demethylases, Tet1 and Tet2, were also expressed higher in the sphere, suggesting changes in DNA methylation during sphere formation [25]. In agreement with this observation, bisulfite sequencing evaluating the methylation status in the promoter regions of Oct4, Nanog, and Sox2 revealed that the methylation in CE spheres was lower than those in monolayer cells (Fig. 4B), indicating these genes were more transcriptionally activated than monolayer cells. Cdh1 and Epcam, which are beneficial to iPS cell generation [19,26], were higher in the CE sphere. However, the difference could result from down-regulation of Cdh1 and Epcam in the monolayer due to the presence of transforming growth factor-β (TGF-β) in serum-containing medium. To rule out this possibility, we grew CE cells in the same serum-containing medium for monolayer culture, but in ultra-low attachment plates. Under such a condition, CE cells formed spheres, and Cdh1 and Epcam were still significantly expressed higher in the spheres (Supplementary Fig. S1; Supplementary Data are available online at www.liebertpub.com/scd). We then checked the expression of other MET genes in the CE culture. Genes encoding TGF-β pathway members (TGFB1, TGFB2, TGFBR1, Zeb1, Zeb2, and Snail, except for Slug) were all upregulated by sphere formation, whereas tested epithelial genes (ZO-1 and OCLN) and BMP pathway members (BMPR2, SMAD1, and SMAD4) were also upregulated. This suggests a BMP-driven MET could occur during sphere formation similar to the initiation phase of fibroblast reprogramming to pluripotency [19]. Together, these findings support the notion that sphere formation induces MET. We hypothesize that this transition may be conducive to iPS cell generation through a sequential EMT–MET mechanism as described previously [27,28].

In this study, we show sphere formation partially reprograms CE cells, and provides an iPS reprogramming advantage. Our observation may be applicable to other cell types such as fibroblasts. Previous studies have shown that forced growth of fibroblasts into spheres caused MET and induced stem cell/progenitor properties [29,30].

In summary, we demonstrated in this study that through sphere formation, Oct4 alone can reprogram CE sphere-derived cells into pluripotent stem cells. Sphere formation reprograms CE cells to progenitor-like cells with the expression of neural stem cell markers and upregulation of various reprogramming factors compared with the monolayer. These findings suggest a two-step reprogramming scheme, in which the first step of sphere formation induces somatic cells into a partially reprogrammed stage, followed by reduced ectopic input for iPS cell reprogramming.

Acknowledgments

S.H.C. would like to acknowledge Hope for Vision, Research to Prevent Blindness Career Development Award, Foundation Fighting Blindness Career Development Award, and NEI K-08 Career Development Award.

Author Disclosure Statement

Authors declare no conflict of interest.

References

1. Ni A, MJ Wu, Y Nakanishi and SH Chavala. (2013). Facile and efficient reprogramming of ciliary body epithelial cells into induced pluripotent stem cells. Stem Cells Dev 22:2543–2550.
2. Forrest AW, RB Keyser and WH Spencer. (1978). Iridocyclectomy for melanomas of the ciliary body: a follow-up study of pathology and surgical morbidity. Ophthalmology 85:1237–1249.
3. Engin G, C Yilmazli, KN Engin, G Gulkilik and L Bilgic. (2004). Combined cyclectomy-trabeculectomy procedure for refractory glaucoma. Ophthalmic Surg Lasers Imaging 35:507–511.
4. Damato BE. (2012). Local resection of uveal melanoma. Dev Ophthalmol 49:66–80.
5. Reynolds BA and RL Rietze. (2005). Neural stem cells and neurospheres—re-evaluating the relationship. Nat Methods 2:333–336.
6. Pastrana E, V Silva-Vargas and F Doetsch. (2011). Eyes wide open: a critical review of sphere-formation as an assay for stem cells. Cell Stem Cell 8:486–498.
7. Tropepe V, BL Coles, BJ Chiasson, DJ Horsford, AJ Elia, RR McInnes and D van der Kooy. (2000). Retinal stem cells in the adult mammalian eye. Science 287:2032–2036.
8. Cicero SA, D Johnson, S Reyntjens, S Frase, S Connell, LM Chow, SJ Baker, BP Sorrentino and MA Dyer. (2009). Cells previously identified as retinal stem cells are pigmented ciliary epithelial cells. Proc Natl Acad Sci U S A 106:6685–6690.
9. Gualdoni S, M Baron, J Lakowski, S Decembrini, AJ Smith, RA Pearson, RR Ali and JC Sowden. (2010). Adult ciliary epithelial cells, previously identified as retinal stem cells with potential for retinal repair, fail to differentiate into new rod photoreceptors. Stem Cells 28:1048–1059.
10. Colman A and O Dreesen. (2009). Pluripotent stem cells and disease modeling. Cell Stem Cell 5:244–247.
11. Kim JB, V Sebastiano, G Wu, MJ Arauzo-Bravo, P Sasse, L Gentile, K Ko, D Ruau, M Ehrich, et al. (2009). Oct4-induced pluripotency in adult neural stem cells. Cell 136:411–419.
12. Kim JB, H Zaehres, G Wu, L Gentile, K Ko, V Sebastiano, MJ Arauzo-Bravo, D Ruau, DW Han, M Zenke and HR Scholer. (2008). Pluripotent stem cells induced from adult neural stem cells by reprogramming with two factors. Nature 454:646–650.
13. Takahashi K, K Okita, M Nakagawa and S Yamanaka. (2007). Induction of pluripotent stem cells from fibroblast cultures. Nat Protoc 2:3081–3089.
14. Ying QL, J Wray, J Nichols, L Batlle-Morera, B Doble, J Woodgett, P Cohen and A Smith. (2008). The ground state of embryonic stem cell self-renewal. Nature 453:519–523.
15. Okada M, M Oka and Y Yoneda. (2010). Effective culture conditions for the induction of pluripotent stem cells. Biochim Biophys Acta 1800:956–963.
16. Imamura M, K Miura, K Iwabuchi, T Ichisaka, M Nakagawa, J Lee, M Kanatsu-Shinohara, T Shinohara and S Yamanaka. (2006). Transcriptional repression and DNA hypermethylation of a small set of ES cell marker genes in male germline stem cells. BMC Dev Biol 6:34.
17. Western PS, JA van den Bergen, DC Miles and AH Sinclair. (2010). Male fetal germ cell differentiation involves

complex repression of the regulatory network controlling pluripotency. FASEB J 24:3026–3035.
18. Hou P, Y Li, X Zhang, C Liu, J Guan, H Li, T Zhao, J Ye, W Yang, et al. (2013). Pluripotent stem cells induced from mouse somatic cells by small-molecule compounds. Science 341:651–654.
19. Samavarchi-Tehrani P, A Golipour, L David, HK Sung, TA Beyer, A Datti, K Woltjen, A Nagy and JL Wrana. (2010). Functional genomics reveals a BMP-driven mesenchymal-to-epithelial transition in the initiation of somatic cell reprogramming. Cell Stem Cell 7:64–77.
20. Buganim Y, DA Faddah, AW Cheng, E Itskovich, S Markoulaki, K Ganz, SL Klemm, A van Oudenaarden and R Jaenisch. (2012). Single-cell expression analyses during cellular reprogramming reveal an early stochastic and a late hierarchic phase. Cell 150:1209–1222.
21. Chia NY, YS Chan, B Feng, X Lu, YL Orlov, D Moreau, P Kumar, L Yang, J Jiang, et al. (2010). A genome-wide RNAi screen reveals determinants of human embryonic stem cell identity. Nature 468:316–320.
22. Payer B, M Rosenberg, M Yamaji, Y Yabuta, M Koyanagi-Aoi, K Hayashi, S Yamanaka, M Saitou and JT Lee. (2013). Tsix RNA and the germline factor, PRDM14, link X reactivation and stem cell reprogramming. Mol Cell 52:805–818.
23. Feng B, J Jiang, P Kraus, JH Ng, JC Heng, YS Chan, LP Yaw, W Zhang, YH Loh, et al. (2009). Reprogramming of fibroblasts into induced pluripotent stem cells with orphan nuclear receptor Esrrb. Nat Cell Biol 11: 197–203.
24. Maekawa M, K Yamaguchi, T Nakamura, R Shibukawa, I Kodanaka, T Ichisaka, Y Kawamura, H Mochizuki, N Goshima and S Yamanaka. (2011). Direct reprogramming of somatic cells is promoted by maternal transcription factor Glis1. Nature 474:225–229.
25. Bagci H and AG Fisher. (2013). DNA demethylation in pluripotency and reprogramming: the role of tet proteins and cell division. Cell Stem Cell 13:265–269.
26. Li R, J Liang, S Ni, T Zhou, X Qing, H Li, W He, J Chen, F Li, et al. (2010). A mesenchymal-to-epithelial transition initiates and is required for the nuclear reprogramming of mouse fibroblasts. Cell Stem Cell 7:51–63.
27. Liu X, H Sun, J Qi, L Wang, S He, J Liu, C Feng, C Chen, W Li, et al. (2013). Sequential introduction of reprogramming factors reveals a time-sensitive requirement for individual factors and a sequential EMT-MET mechanism for optimal reprogramming. Nat Cell Biol 15:829–838.
28. Di Stefano B, JL Sardina, C van Oevelen, S Collombet, EM Kallin, GP Vicent, J Lu, D Thieffry, M Beato and T Graf. (2013). C/EBPalpha poises B cells for rapid reprogramming into induced pluripotent stem cells. Nature 506:235–239.
29. Su G, Y Zhao, J Wei, Z Xiao, B Chen, J Han, L Chen, J Guan, R Wang, Q Dong and J Dai. (2013). Direct conversion of fibroblasts into neural progenitor-like cells by forced growth into 3D spheres on low attachment surfaces. Biomaterials 34:5897–5906.
30. Liu Y, P Mukhopadhyay, MM Pisano, X Lu, L Huang, Q Lu and DC Dean. (2013). Repression of Zeb1 and hypoxia cause sequential mesenchymal-to-epithelial transition and induction of aid, Oct4, and Dnmt1, leading to immortalization and multipotential reprogramming of fibroblasts in spheres. Stem Cells 31:1350–1362.

Address correspondence to:
Dr. Sai H. Chavala
Department of Ophthalmology
University of North Carolina
5151 Bioinformatics Building, CB #7040
Chapel Hill, NC 27599-7040

E-mail: schavala@med.unc.edu

Received for publication January 30, 2014
Accepted after revision July 14, 2014
Prepublished on Liebert Instant Online July 15, 2014